






Earth's Future



RESEARCH ARTICLE

10.1029/2022EF003337

Projected Changes to Wintertime Air-Sea Turbulent Heat Fluxes Over the Subpolar North Atlantic Ocean

Christopher Barrell¹ , Ian A. Renfrew¹ , John C. King² , Steven J. Abel³ , and Andrew D. Elvidge¹ 

¹School of Environmental Sciences, University of East Anglia, Norwich, UK, ²British Antarctic Survey, Cambridge, UK,

³Met Office, Exeter, UK

Key Points:

- The climate model HadGEM3-GC3.1 simulates historic sea ice and turbulent heat fluxes reasonably well, with improvements at higher resolution
- Upward turbulent heat fluxes are predicted to reduce, particularly in the Labrador and Irminger Seas and the interior of the Nordic Seas
- Changes in local heat flux maxima are largely governed by ice edge retreat, while overall a reduction in ocean heat loss is projected

Supporting Information:

Supporting Information may be found in the online version of this article.

Correspondence to:

C. Barrell,
c.barrell@uea.ac.uk

Citation:

Barrell, C., Renfrew, I. A., King, J. C., Abel, S. J., & Elvidge, A. D. (2023). Projected changes to wintertime air-sea turbulent heat fluxes over the subpolar North Atlantic Ocean. *Earth's Future*, 11, e2022EF003337. <https://doi.org/10.1029/2022EF003337>

Received 16 NOV 2022
Accepted 31 MAR 2023

Author Contributions:

Conceptualization: Christopher Barrell, Ian A. Renfrew
Formal analysis: Christopher Barrell
Funding acquisition: Ian A. Renfrew
Investigation: Christopher Barrell
Methodology: Christopher Barrell, Ian A. Renfrew, Andrew D. Elvidge
Supervision: Ian A. Renfrew, John C. King, Steven J. Abel, Andrew D. Elvidge
Visualization: Christopher Barrell
Writing – original draft: Christopher Barrell

© 2023 The Authors. Earth's Future published by Wiley Periodicals LLC on behalf of American Geophysical Union. This is an open access article under the terms of the [Creative Commons Attribution License](https://creativecommons.org/licenses/by/4.0/), which permits use, distribution and reproduction in any medium, provided the original work is properly cited.

Abstract In wintertime over the subpolar North Atlantic Ocean (SPNA), the strongest surface sensible and latent heat fluxes typically occur just downstream of the sea-ice edge. The recent retreat in Arctic wintertime sea ice is changing the distribution of these turbulent heat fluxes, with consequences for the formation of the dense waters that feed into the Atlantic Meridional Overturning Circulation. Projections of turbulent heat flux over the SPNA are investigated using output from the HadGEM3-GC3.1 climate model, produced as part of the sixth phase of the Coupled Model Inter-Comparison Project. Comparison of two model resolutions (MM: 60 km atmosphere—1/4° ocean and HH: 25 km—1/12°) shows that the HH configuration more accurately simulates historic sea ice and turbulent heat flux distributions. The MM configuration tends to produce too much sea ice in the SPNA, affecting the turbulent heat flux distribution; however, it displays improved performance during winters with less sea ice, increasing confidence in future projections when less sea ice is predicted. Future projections are presented for low (SSP1-2.6) and high (SSP5-8.5) emissions pathways. The simulations agree in predicting that, with climate change, the SPNA will see reductions in wintertime sea ice and air-sea turbulent fluxes later in the 21st century, particularly in the Labrador and Irminger Seas and the interior of the Nordic Seas, and a notable reduction in their decadal variability. These effects are more severe under the SSP5-8.5 pathway. The implications for SPNA ocean circulation are discussed.

Plain Language Summary In winter over the subpolar North Atlantic Ocean a large amount of heat is transferred from the ocean to the air just off the sea ice. This heat loss drives water mass changes in the ocean, which, in turn, helps drive global ocean circulation. The subpolar North Atlantic is rapidly warming due to fossil fuel emissions, resulting in a large reduction of sea ice that may further impact global climate. We look at predictions of future sea ice loss and its effects on air-sea heat exchange using some of the latest climate simulations that represent the atmosphere and the ocean at high spatial resolution. These simulations do reasonably well at reproducing the historic climate of the region, so we have some confidence that they are suitable for making predictions of future conditions. We investigate future projections for low and high emissions scenarios, finding that ocean heat loss to the atmosphere will reduce, particularly in the Labrador, Irminger and interior of the Nordic Seas, and by a greater amount under the high emissions scenario. How this could affect the ocean is discussed.

1. Introduction

The air-sea exchange of heat and moisture over the subpolar North Atlantic (SPNA) plays a crucial role in atmosphere-ocean coupling and consequently ocean circulation (Buckley & Marshall, 2016). The strongest surface sensible and latent heat fluxes occur during cold-air outbreaks, which account for 60%–80% of wintertime oceanic heat loss in the SPNA (Papritz & Spengler, 2017). These turbulent heat fluxes cool the surface waters and promote water mass transformation and convective overturning, thus playing a crucial role in the Atlantic Meridional Overturning Circulation (AMOC)—a key component of the global climate system (Schmitz, 1995; Talley, 1996; Zhang et al., 2019). The AMOC brings warm, salty water from the Gulf of Mexico northwards into the SPNA, where it becomes colder and denser and then sinks, to be exported southwards as North Atlantic Deep Water (Buckley & Marshall, 2016). The release of oceanic heat into the atmosphere in the SPNA has a profound effect on the climate of northwest Europe, raising air temperatures by as much as 6°C compared to Pacific maritime climates at a similar latitude (Palter, 2015).

Writing – review & editing: Christopher Barrell, Ian A. Renfrew, John C. King, Steven J. Abel, Andrew D. Elvidge

Over 30 years ago, Aagaard and Carmack (1989) suggested that the Greenland and Iceland Seas were “delicately poised” in their ability to sustain convection. Since their publication, conditions in the Arctic and nearby subpolar regions have changed substantially. Most notably, a rapid decline of sea ice has been observed (Cavalieri & Parkinson, 2012; Comiso et al., 2008; Parkinson & Cavalieri, 2008), raising concern that in summertime the Arctic will be ice free (<1 million km²) within a couple of decades (Overland & Wang, 2013). Parkinson and Cavalieri (2008) showed that while summer sea ice has declined in the Greenland, Iceland and Irminger Seas by 11.4%/decade ($\pm 4.3\%$), winter sea ice has also declined by 10.0%/decade ($\pm 2.5\%$) over the period 1979–2006. More recently, Sévellec et al. (2017) found that annual mean Arctic sea-ice area has reduced by around 20% over the period 1979–2014.

Moore et al. (2015) showed that wintertime sea-ice retreat in the Iceland and Greenland Seas, along with different rates of warming for the ocean and the atmosphere, has resulted in reductions of around 20% in the magnitude of air-sea turbulent heat fluxes in these seas between 1979 and 2014. They also demonstrate that further decreases in atmospheric forcing will likely reduce ventilation of mid-depth waters in the Greenland Sea and decrease the supply of the densest waters into the lowest limb of the AMOC. Furthermore, a retreating ice cover in the vicinity of the region's boundary currents is also responsible for recent changes in the spatiotemporal variability of air-sea heat fluxes (Moore et al., 2022); who suggested that a reorganisation of *where* water mass transformation occurs is underway, with increased turbulent heat fluxes observed over the boundary currents in the SPNA, where retreating sea ice has exposed them to the atmosphere (e.g., see Våge et al., 2018). These findings beg important questions: what is the future of sea ice and air-sea turbulent heat fluxes in the SPNA region, and what are the ramifications of these predicted changes for the AMOC?

There is evidence to suggest that the AMOC has already slowed to some extent. The AMOC has been measured by the RAPID array at 26.5°N since 2004 and, despite significant variability, the observed volume transport has been ~15% lower since 2008, than in the 2004–2008 period (Smeed et al., 2018). Other studies that use proxies or models also suggest that a gradual slowdown of the AMOC is underway (e.g., Caesar et al., 2018; Rahmstorf et al., 2015). Coupled climate models show it is likely to continue declining in response to anthropogenic climate change over the 21st century (Fox-Kemper et al., 2021).

In the latest multi-model, multi-resolution ensemble from the Coupled Model Intercomparison Project Phase 6 (CMIP6), a set of higher resolution simulations (HighResMIP) show that the AMOC and northward heat transport to the SPNA tends to become stronger as ocean model resolution is increased and this agrees better with RAPID observations (Chassignet et al., 2020; Roberts et al., 2020). Further, the higher resolution ocean models (1/12° to 1/4°) predict larger declines in the AMOC than the more typical lower resolution (1°–2.5°) models, suggesting a potentially greater risk is posed by climate change than previously anticipated (Roberts et al., 2020). Higher resolution models also enable the analysis of more complex smaller scale changes to air-sea interactions. For example, Wang et al. (2020) identified in high resolution ocean simulations a mechanism where sea ice retreat leads to intensified heat transport to the Arctic Ocean through Fram Strait, potentially contributing to the “Atlantification” of the Arctic.

This study makes use of output from HadGEM3-GC3.1, one of the better performing CMIP6 members in terms of AMOC representation (Heuzé, 2021; Hirschi et al., 2020; Roberts et al., 2020) and Arctic sea-ice mass budget (Keen et al., 2021), to explore the future of air-sea turbulent fluxes in the SPNA. Note however, there is a large spread in sea-ice area and mass across the CMIP6 ensemble, both in historic and future simulations (Notz & SIMIP Community, 2020). We investigate output from several single CMIP6 members (MM and HH resolution), taking a storyline approach in order to compare several plausible and physically consistent simulations of the future (Shepherd et al., 2018).

We address several key questions:

- How well does the model simulate climatological sea ice and air-sea turbulent heat fluxes, and how does this vary with model resolution?
- How are these fluxes projected to change over the course of the 21st century?
- What are the implications for the formation of dense waters in the subpolar North Atlantic?

2. Data and Methods

2.1. ERA5

To provide a quasi-observational data set by which to evaluate the historic model runs we use the European Centre for Medium-Range Weather Forecasts (ECMWF) Reanalysis version 5 (ERA5). At the time of writing,

Table 1
Overview of the Model Simulations Evaluated

HadGEM3-GC3.1 configuration	Atmosphere grid length (km)	Ocean grid length	Run length (years)	Period
MM-historical	60	1/4°	64	1950–2013
HH-hist-1950	25	1/12°	64	1950–2013
HH-control-1950	25	1/12°	100	1950–2049 (nominal)
MM-SSP1-2.6	60	1/4°	85	2015–2099
MM-SSP5-8.5	60	1/4°	85	2015–2099
HH-HighRes-future (SSP5-8.5)	25	1/12°	35	2015–2049

Note. Details on model configurations and forcings applied are in Andrews et al. (2020) for the historical runs, Roberts et al. (2019) for the control run and Eyring et al. (2016) for the future scenarios.

the data is available in two parts: 1979–present, which has significantly more satellite observations available (Hersbach et al., 2019); and the 1950–1978 preliminary back extension, which has greater uncertainty due to fewer available observations (Bell et al., 2020). ERA5 offers several advantages compared to its predecessor, ERA-Interim, which was used by Moore et al. (2012) to document the climatological air-sea fluxes over the SPNA. These include an improved model configuration (IFS Cycle 41r2), increased resolution (~30 km), and the extended record back to 1950 that conveniently matches the available period for the HadGEM3-GC3.1 High-ResMIP historical simulations. In Section 3 we use ERA5 data for winters beginning in 1950–2013 for direct comparison to available model winters, while in Section 4 the time period used is 1950–2019.

An evaluation of ERA5 against in-situ observations in the Iceland and Greenland Seas showed that it generally performs very well in that region, albeit with less accuracy over the marginal ice zone than over the open ocean (Renfrew et al., 2021). However, a comparison against observations made north of Svalbard showed that while radiative flux biases are lower in ERA5 than other reanalysis products, due to improvements in cloud simulation, considerable biases in turbulent heat fluxes over sea ice remain (Graham et al., 2019).

2.2. HadGEM3-GC3.1

To investigate the future evolution of air-sea turbulent heat fluxes over the course of the 21st century we use output from the Hadley Centre Global Environment Model 3—Global Coupled version 3.1 (HadGEM3-GC3.1) at medium-medium (MM; Williams et al., 2017; Andrews et al., 2020) and high-high (HH; Roberts, 2017; Roberts et al., 2019) atmosphere-ocean resolutions of 60 km—1/4° and 25 km—1/12°, respectively. The MM model output was configured for submission to CMIP6 (Eyring et al., 2016) and the HH model output was configured for HighResMIP (Haarsma et al., 2016).

The atmospheric component has science configuration GA/GL7.1 (Walters et al., 2019), with 85 vertical levels to a height of 85 km and a rectilinear grid. The ocean component, GO6 (Storkey et al., 2018), has 75 vertical levels and a curvilinear tripolar grid. At MM resolution the ocean model is eddy-permitting, while at HH resolution it could be described as eddy-rich. The sea ice component, GSI8.1 (Ridley et al., 2018) uses the same grid as the ocean. Data on the tripolar grid system, particularly at high resolution, poses a nontrivial challenge to utilize. We transformed all output onto a regular latitude-longitude 0.25° by 0.25° grid to match that utilized for ERA5 and allow straightforward comparisons and statistical analyses using the Climate Data Operator (CDO) suite of tools.

The model simulations analyzed are listed in Table 1. Verification of HadGEM3-GC3.1 output is performed through comparison of historic simulations (1950–2013, with observed historical climate forcing applied; see Andrews et al., 2020) against climatological values from ERA5. The HH model is computationally expensive and the future simulation stops in 2049. Consequently, we also include the HH control run (1950–2049 which has constant 1950 climate forcing; see Roberts et al., 2019) in our evaluation. All the future runs are forced using the standardised time varying CMIP6 forcings detailed in Eyring et al. (2016), as specified by alternative future shared socioeconomic pathways (SSPs). In this study only two of the five pathways are analyzed, SSP1-2.6 and SSP5-8.5. The key factor in each scenario is their long-term global average radiative forcing levels, which are 2.6 and 8.5 Wm⁻² respectively, as denoted in the acronyms. These two pathways represent the extremes of the suggested range of possible future scenarios. For the MM configuration both pathways are evaluated to 2100, but

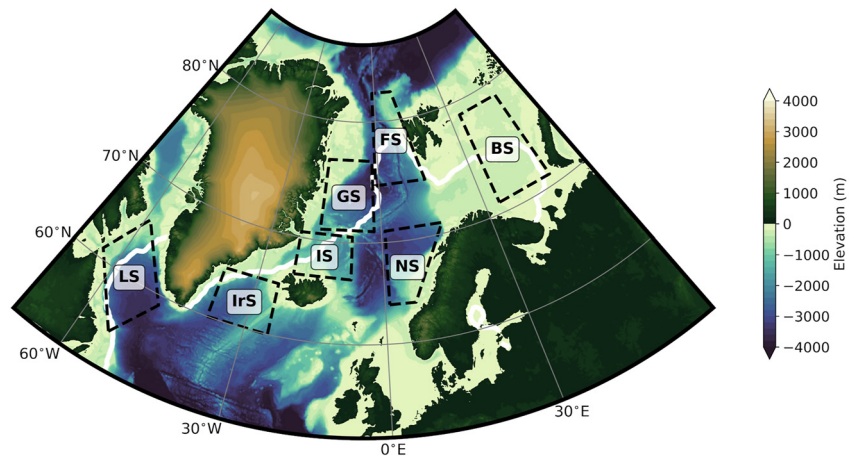


Figure 1. Map of the subpolar North Atlantic, with bathymetry and topography shaded. The study regions outlined by the black dashed lines are Labrador Sea (LS), Irminger Sea (IrS), Iceland Sea (IS), Greenland Sea (GS), Fram Strait (FS), Norwegian Sea (NS), and Barents Sea (BS). The thick white line represents the ERA5 winter mean (1950–2020) 15% sea ice concentration contour.

the HH future run is only available to 2050 and with SSP5-8.5 forcing. As only one model realisation is available for the HH future simulation, for parity we primarily use only the first realisation of the MM simulations. To check the validity of this decision four realizations of the MM historical model were compared and we found little difference between them when considering the climatological winter means of interest to this study (not shown).

2.3. Methodology

For the purposes of this study, the SPNA is defined as the non-land area from 70°W to 60°E, and 50°N to 85°N—see Figure 1. Within the SPNA we define seven study regions (similar to Papritz & Spengler, 2017), namely the Greenland, Iceland, Norwegian, Barents, Irminger and Labrador Seas, and Fram Strait west of Svalbard. We use monthly averaged data from ERA5 and HadGEM3-GC3.1 to calculate extended winter (here defined as December to March) mean values, denoted henceforth by the year in which the winter started.

To analyze sea-ice conditions we compute the average grid cell sea-ice concentration as output by the model for each study region. This is not converted to sea-ice area as we focus on the fraction of sea ice over time in each region allowing us to easily compare them, rather than the absolute area of sea ice.

3. Evaluation of Historic Simulations

3.1. Spatial Distribution of Sea Ice and Turbulent Heat Fluxes

Figure 2 displays the spatial distribution of wintertime-mean meteorological fields over the climatological period of 1950–2013 for ERA5 and the HadGEM3-GC3.1 HH and MM models (i.e., HH historical; MM historical). As ERA5 is very similar to its predecessor ERA-Interim, it follows that there is very close agreement with previous climatologies (e.g., Moore et al., 2012) in the spatial distribution of 2 m air temperature (T_a), mean sea level pressure (MSLP) and the sum of upward sensible and latent heat, the total turbulent heat flux (THFX). The HH historical simulation shows generally good spatial agreement with ERA5. However, it exhibits too much sea ice in the Iceland and Greenland Seas. This is due to simulated years when these regions were largely covered by sea ice (i.e., when there is an Odden Ice tongue, see Wadhams & Comiso, 1999), which leads to the 25% sea ice concentration contour being too far east. Conversely, the ice edge is reasonably accurate in the Fram Strait and Barents Sea regions in the HH historical model, though the ice concentration is too low east of Svalbard. The MSLP in the HH historical output agrees very well with ERA5, especially in the position and depth of the Icelandic Low. The T_a and THFX fields also generally agree well with the climatology, although the magnitude of the fluxes is too high near the ice edge in the western Labrador Sea, Fram Strait and the northern Irminger Sea. This is despite a good representation of T_a , MSLP and 10-m winds (not shown) in these regions, which suggests it may

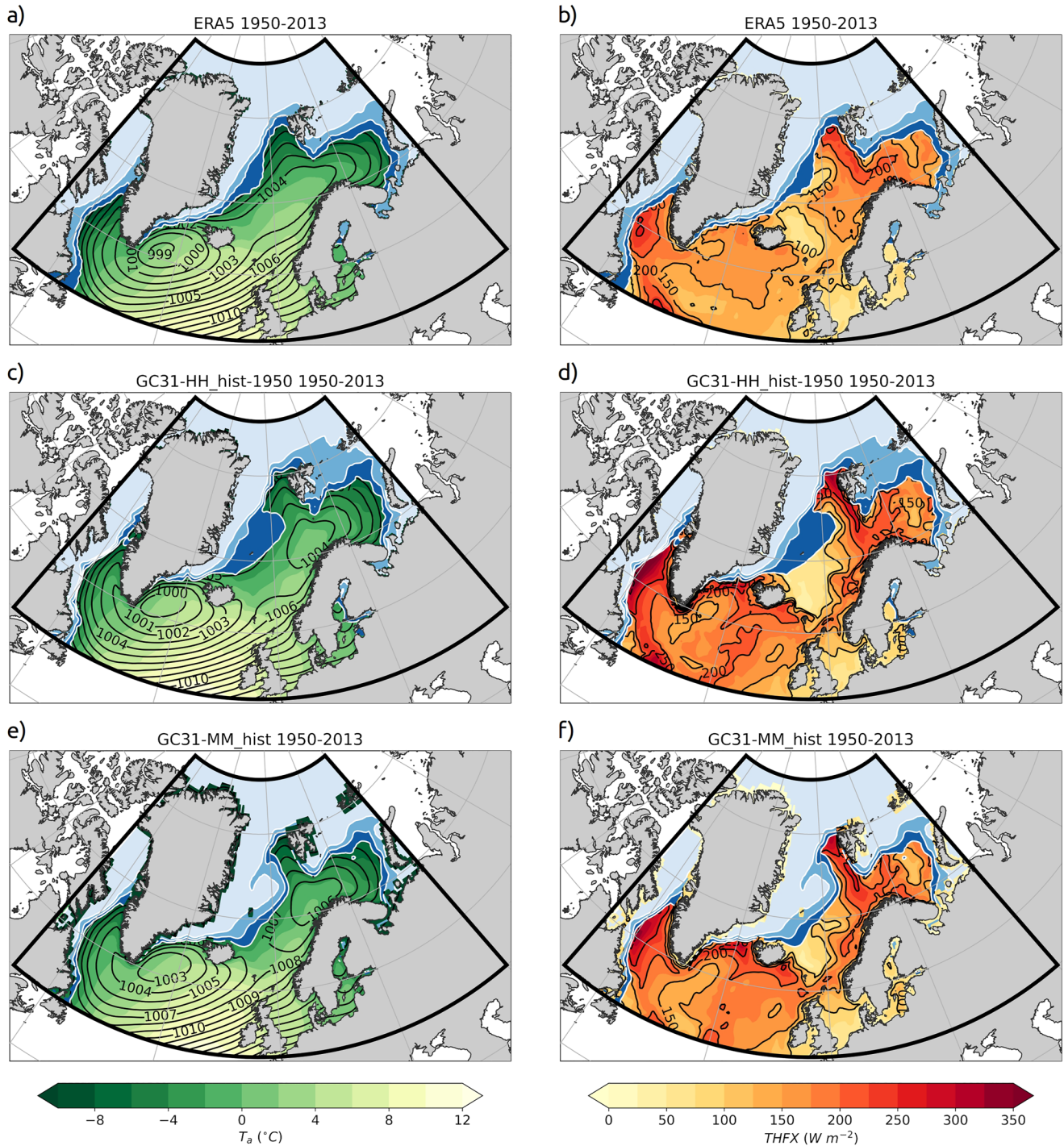


Figure 2. Spatial distribution of winter-mean fields (DJFM from 1950 to 2013) of sea-level pressure (black contours) and 2 m air temperature (colored shading) in the left column; and total turbulent heat flux (colored shading) in the right column. In all panels sea-ice fraction is overlaid via blue shaded contours at 25%, 50%, and 75%. Panels are for ERA5 reanalysis in (a) and (b); HadGEM3-GC3.1 HH historical in (c) and (d); and HadGEM3-GC3.1 MM historical in (e) and (f).

be related to the surface exchange parameterization over the marginal ice zone (see Elvidge et al., 2016, 2021; Renfrew et al., 2019). In the Iceland and Greenland Seas, THFX in the HH historical is slightly lower than ERA5.

The MM historical run captures the same climatological features but is different to the HH run in key places. It simulates far too much sea ice in the Iceland and Greenland Seas, with these regions being mostly ice covered; although, the northward position of the ice edge in the Fram Strait and Barents Sea is in good agreement with

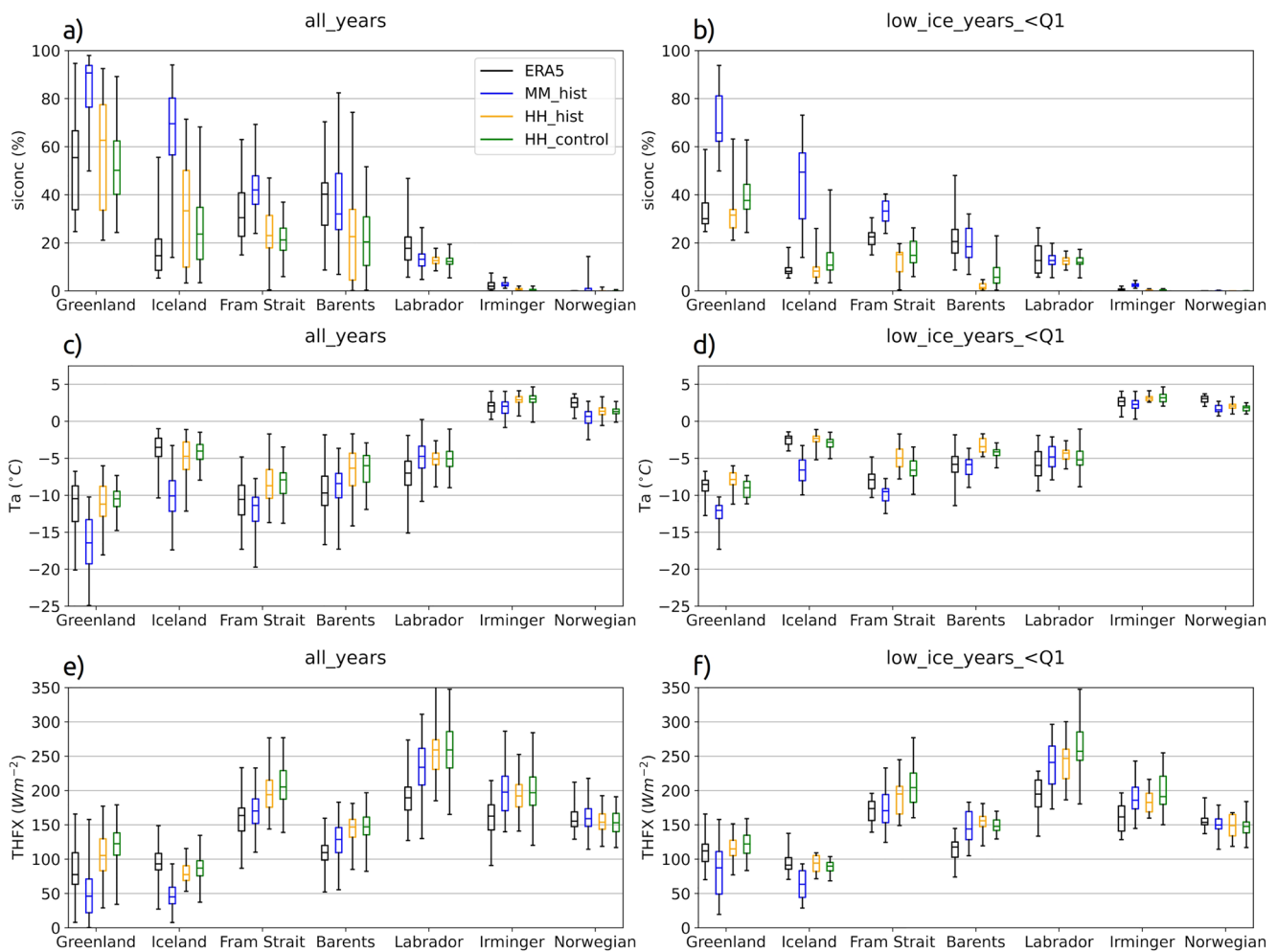


Figure 3. Box and whisker plots for surface variables across seven regions, using output from ERA5 (1950–2013), and the models MM historical (blue), HH historical (orange) and HH control (green) simulations as marked (see also Table 1). The statistics are for DJFM, with the left column displaying data for all years and the right column displaying data for low ice years. The panels are for sea-ice concentration in (a) and (b), air temperature (T_a) in (c) and (d) and total surface heat flux (THFX) in (e) and (f).

ERA5. The Icelandic Low is too shallow (by ~ 3 mb) representing a notable difference in the representation of the atmospheric circulation and wind speeds over the SPNA. This may be due to underrepresentation of extratropical cyclones; a known deficiency of lower resolution atmospheric models (e.g., Jung et al., 2006). The surface air temperature field in the MM historical run is very similar to the HH run and agrees well with ERA5. The magnitude of peak turbulent heat fluxes in the Labrador Sea and Fram Strait is slightly lower than the HH model and closer to ERA5. However, the substantial amounts of extra sea ice in the Iceland, Greenland and Irminger Seas leads to incorrect THFXs in these regions.

The similarities between the historical simulations include THFXs that are too low in the Iceland and Greenland Seas, and too high in the Irminger and Labrador Seas and Fram Strait. In the Barents Sea the models show good agreement with ERA5, though the concentration of sea ice east of Svalbard is too low in the HH historical simulation. Both resolutions simulate the magnitude of Norwegian Sea THFX reasonably well but with an incorrect east-west gradient due to the overly low fluxes to the west.

3.2. Regional Analysis

Analysis of regional statistics for selected surface conditions enables a more quantitative evaluation of the simulations' veracity (Figure 3). It demonstrates that the MM historical model produces far too much sea ice in the

Greenland and Iceland Seas with median sea-ice concentrations of approximately 90% and 70% respectively, compared with 50% and 10% in ERA5 (Figure 3a). This bias in sea-ice fraction leads to a cold bias in T_a of over 5°C (Figure 3c) and consequently a negative bias in THFX (Figure 3e). Despite reasonable agreement with ERA5 in the other regions, overall, the MM historical provides a comparatively poor reproduction of air-sea interactions in the SPNA.

In contrast, the HH historical run has better agreement with ERA5 over the Greenland and Iceland Seas, although the interquartile range in sea ice is too large and somewhat biased high for the Iceland Sea (Figure 3a). As seen in the spatial plots (Figure 2), the HH historical tends to underestimate the amount of sea ice a little in Fram Strait and the Labrador Sea, while it is more significantly underestimated in the Barents Sea. The consequence is positive biases in THFX in these regions (Figure 3e). The Norwegian and Irminger Seas are mostly ice free, which the models reproduce well. Note the HH control largely corroborates the HH historical simulations results.

The differences between model and reanalysis T_s , T_a , and THFX are qualitatively similar across model resolution and are seemingly related to errors in the sea-ice distribution. The HH model displays notably higher T_s in all regions compared to the MM simulation (not shown), likely linked to the increased northward heat transport into the SPNA in the higher resolution configuration (Roberts et al., 2020). The result is enhanced THFX in the HH historical and the HH control simulations, with a larger bias in the Fram Strait and Barents and Labrador Seas than the MM historical. However, overall, the HH surface variables correspond more closely to ERA5 than those from the MM run, that is, the higher resolution improves their fidelity.

3.3. Conditional Sampling by Sea Ice Extent

It is evident that the sea ice in these climate simulations is a major source of variability and error. This prompts the question: are the models more accurate when there is less sea ice? If true, this would provide confidence in future projections when less sea ice is expected (e.g., IPCC, 2021). We address this question by conditionally sampling the historical simulations and analyzing model performance during “low” and “high” ice years. These are defined independently for each data set to enable a statistical assessment, rather than from the observational record alone, using conditional sampling to select the winters that have lower (<Q1) or higher (>Q3) than average sea-ice extent over the whole SPNA. This conditional sampling method follows a storyline approach (Shepherd et al., 2018) and is justified by the high confidence of there being less Arctic sea ice in the future (IPCC, 2021).

In low ice years (Figure 3b), the HH historical simulation shows very good agreement with ERA5 in the Iceland and Greenland Seas, while the MM historical has far too much sea ice (despite the conditional sampling). The HH control run also corresponds well to ERA5 in these regions. In Fram Strait, the HH historical does not produce enough sea ice, while the MM historical model produces too much. Both the HH historical and control runs simulate too little sea ice in the Barents Sea, possibly linked to the stronger northward North Atlantic Ocean heat transport in the HH configuration compared to the MM (Roberts et al., 2020). All the simulations are accurate during low ice years in the Labrador Sea, albeit with insufficient variability. Generally, the HH control configuration tends to produce more sea ice than the HH historical for each region, as would be expected with constant 1950s forcing. Over the SPNA generally, the HH historical simulation represents THFX closer to ERA5 than the MM historical during low ice years (Figure 3f), albeit with too little sea ice in Fram Strait and the Barents Sea. These results provide greater confidence that the HH future projections will be comparatively skillful for the SPNA, though care must be taken to consider model uncertainty.

In the high ice years (not shown), the MM historical model invariably produces near-continuous ice cover over the Greenland Sea study region, however, in ERA5 the wintertime mean ice cover is typically 60%–80%. The insulative layer of sea ice mostly prevents model air-sea interaction in this region. This problem is also evident over the Iceland Sea region: the MM historical simulates the range of mean sea ice concentration to be 70%–90%, while in ERA5 it is 10%–50%.

The spatial patterns of sea ice and THFX during the low ice years highlight the systematic model errors described above (Figure 4). The HH historical displays a substantial lack of sea ice in the Barents Sea region, with the model tending to produce open water north of Svalbard and excessive THFX. Otherwise, the HH historical is generally in good agreement with ERA5, albeit with a slightly retreated ice edge around Greenland (resulting in a misplacement of THFX maxima). The MM historical simulation produces an Odden Ice Tongue feature even in low ice years, representing a large error in the model sea ice in the Iceland and Greenland Seas. However, elsewhere the

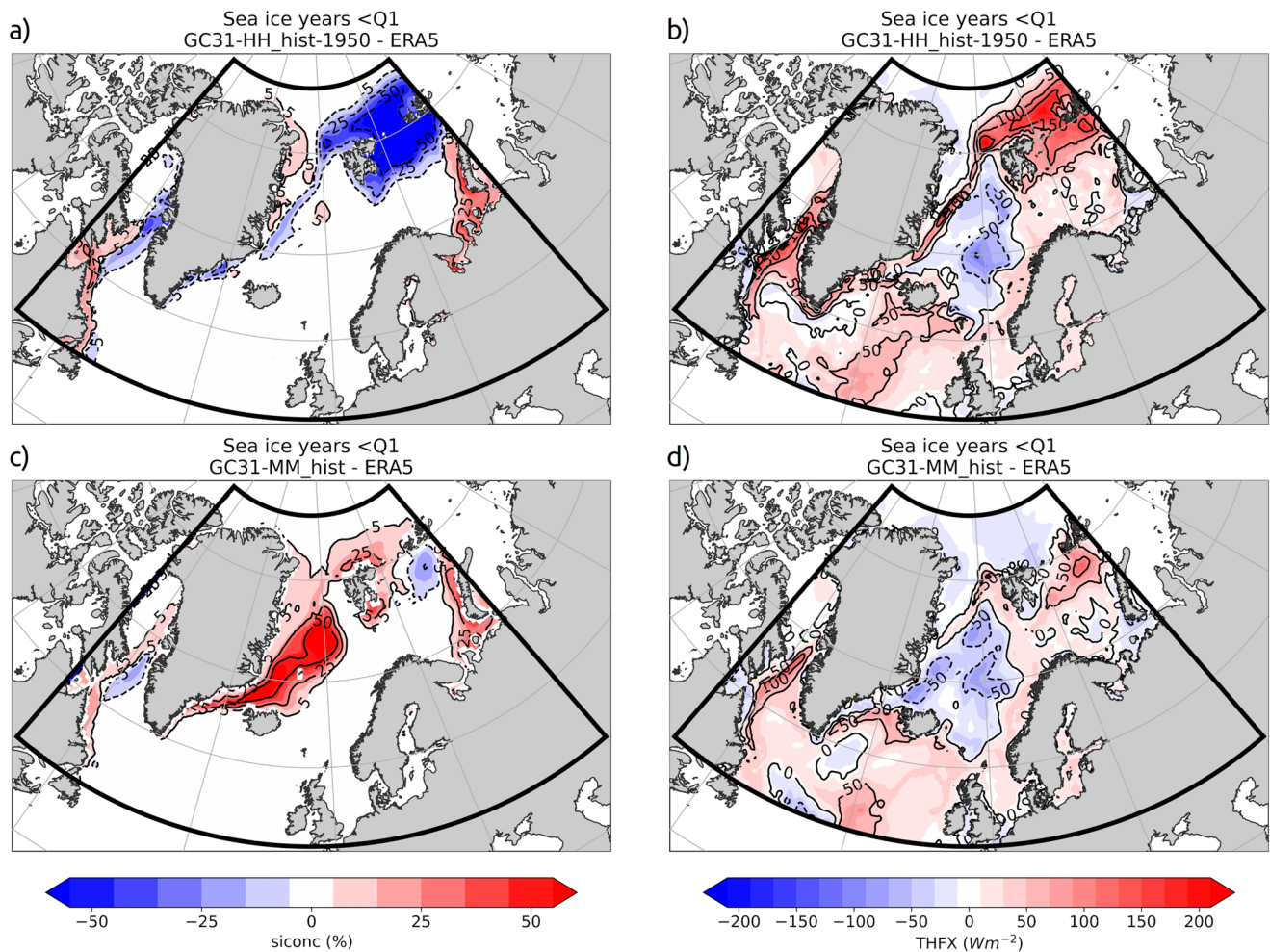


Figure 4. Spatial difference plots compared to ERA5 for DJFM HadGEM3-GC3.1 HH historical in (a) and (b) and HadGEM3-GC3.1 MM historical in (c) and (d). The left column displays sea ice concentration, and the right column THFX. Each product has been conditionally sampled based on winter mean sea ice concentration in the subpolar North Atlantic region in each model, so that the lower quartile represents the composited “low ice years.”

sea ice is in good agreement with ERA5, with the position of the sea ice edge better reproduced than the HH historical in the Barents Sea.

Overall, the boxplots appear to show that the HH model simulates THFX more accurately than the MM model in all the study regions except for the Barents Sea (Figure 3); yet the spatial difference plots reveal that there are both strengths and weaknesses in the HH simulation (Figure 4). The sea ice extent in the Iceland and Greenland Seas is comparatively accurate during low ice years, but this is countered by a substantial lack of sea ice in the Barents Sea. Both model resolutions exhibit a tendency to produce a sea ice edge i.e., too far retreated in the Labrador Sea.

4. Evaluation of Future Projections

4.1. Decadal Time Series

To analyze the future projections, time series of decadal quantities are presented which show model trends and variability (Figure 5). Note we omit the Norwegian Sea region from this plot as sea ice has little influence there. Winter sea ice is projected to almost entirely disappear from the SPNA over the course of the 21st century under SSP5-8.5 forcing (Figure 5a). The HH and MM resolution simulations under this forcing are consistent in their trend and converge by the 2040s. Although there are notable discrepancies during the 2020s, for example, a persistence of the large bias in MM historical sea ice extent in the Iceland and Greenland Seas, resulting in an unrealistic deviation from the ERA5 observed timeseries.

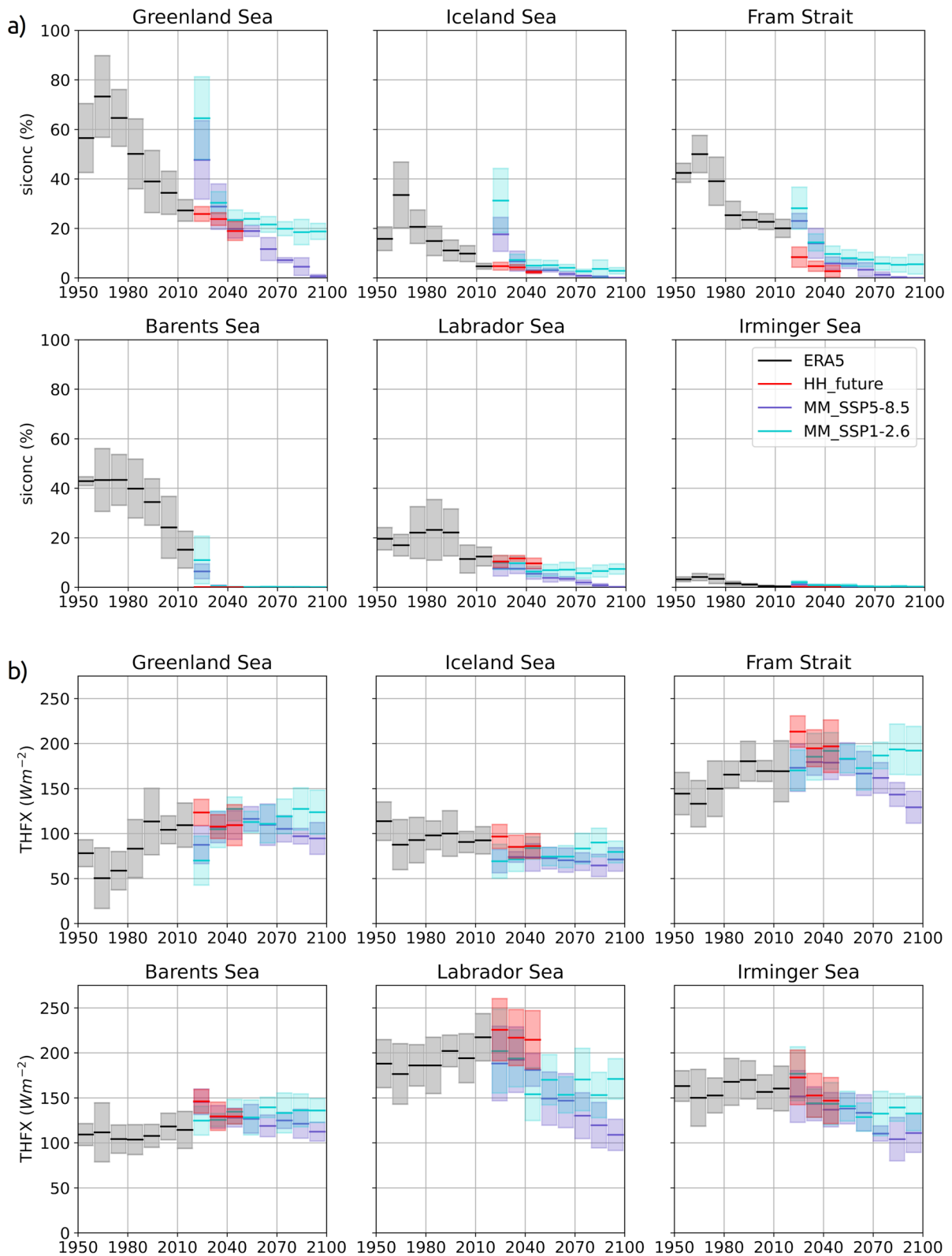


Figure 5. Regional time series of (a) sea ice concentration (%) and (b) total turbulent heat flux ($W m^{-2}$) showing decadal means (thick lines) and decadal variability indicated by ± 1 standard deviation (shaded regions) for the historical ERA5 record (1950–2020; black), and the future simulations from HadGEM3-GC3.1: HH future (2020–2050; SSP5-8.5 forcing; red), MM SSP1-2.6 (2020–2100; cyan), and MM SSP5-8.5 (2020–2100; purple) for DJFM.

Earlier we suggested that as atmosphere and ocean temperatures increase, resulting in reduced winter sea ice, climate projections for the SPNA will benefit from reduced uncertainty as the variability associated with sea-ice is absent. Figure 5a is consistent with this suggestion. It generally shows smaller standard deviations from the 2040s onwards in the MM simulations. Our results are consistent with those of the CMIP6 multi-model mean, which shows wintertime sea ice reducing substantially and the Arctic becoming ice free (ice area <1 million km²) in summer under emissions scenarios SSP2-4.5 and above (Notz & SIMIP Community, 2020); or a slowing rate of decline and stabilization of sea ice toward 2100 for the Greenland, Iceland and Labrador Seas and the Fram Strait region for the SSP1-2.6 scenario.

Figure 5b shows decadal timeseries of THFX over the SPNA, which is projected to decrease from around 2030 through the 21st century under SSP5-8.5, with pronounced reductions in the Labrador and Irminger Seas and Fram Strait. The HH future simulation generally corroborates the MM SSP5-8.5 simulation from the 2030s, as for sea ice, though with slightly higher THFX. As such, a reduction in dense water formation in the SPNA would be anticipated under SSP5-8.5. Under SSP1-2.6, there are also reductions in THFX in the Labrador and Irminger Seas. However, in the Greenland and Barents Seas, and in Fram Strait, the different scenarios yield different trends; under SSP1-2.6, there is a small increase in THFX over the course of the century, while under SSP5-8.5 there is a sizable reduction. The divergence in response here arises from the interplay between the retreating sea ice exposing relatively warm ocean currents to the atmosphere (Moore et al., 2022) and the degree to which the mean air-sea temperature difference changes.

The impact of the influence of differential warming in the atmosphere and the ocean can be visualized via $\Delta T = T_s - T_a$ and decadal trends of this are very similar to the THFX trends (Figure S1 in Supporting Information S1). Under the high emissions scenario, SSP5-8.5, ΔT shows generally good agreement between the HH and MM models in a downward trend to 2050, with substantial further decreases to 2100. Under the less severe SSP1-2.6 emissions scenario ΔT is projected to remain relatively stable during the period 2050 to 2100 across the SPNA. A closer examination for individual seas reinforces that the differential atmosphere-ocean warming is critical to explaining the THFX trends in the different seas. The changes seen suggest that the SPNA is entering a new, more homogeneous regime, whereby the disappearance of ice results in increasingly similar T_a and T_s . In regions where more ice is lost, the larger the change in temperature over the 21st century, particularly in the Greenland Sea and the Fram Strait, where, compared to 1950s observations, mean T_a is projected to be roughly 10°C–15°C higher by 2100 between SSP1-2.6 and SSP5-8.5 (not shown). Such a temperature increase represents a substantial change in atmospheric forcing of the ocean.

It is worth noting that loss of wintertime sea ice leads to a noticeable reduction in the decadal variability of THFX. We have also examined the surface sensible and latent heat flux trends separately (Figure S2 in Supporting Information S1). Sensible heat fluxes are predicted to significantly decline under SSP5-8.5 forcing and remain relatively stable toward the end of the 21st century under SSP1-2.6 forcing as a result of weak cold-air outbreaks in the future (Papritz & Spengler, 2017). In contrast, increasing latent heat fluxes are projected under both warming scenarios in the Greenland and Barents Seas and in the Fram Strait. We hypothesize that increasing latent heat fluxes in these regions is a “fingerprint” of the exposure of more ocean to relatively dry cold-air outbreak air masses (Papritz & Spengler, 2017). See Supporting Information S1 for more details.

4.2. Spatial Distribution During the Mid and Late 21st Century

In the decade 2040–2049 there is good qualitative agreement between the model simulations in the retreat of the ice edge in the Iceland and Greenland Seas, and to the north of Fram Strait and the Barents Sea (Figure 6). The T_a field is also similar between the three projections, though with the warmer air advanced further north in the simulations under SSP5-8.5 forcing. Atmospheric warming in the SPNA is greater at higher latitudes, by up to 5°C, where sea ice has retreated north of Svalbard relative to the ERA5 base period of 2000–2019, representing a large Arctic Amplification of global warming (Serreze & Barry, 2011).

The MSLP fields display notable differences between the simulations. HH future features a deep mean Icelandic Low of around 998 mbar, MM SSP5-8.5 is shallower at around 1002 mbar, while MM SSP1-2.6 is much shallower at 1007 mbar suggesting the scenario is affecting the mean circulation. The SSP5-8.5 pathway resulting in a stronger Icelandic Low than the SSP1-2.6 pathway by the middle of the 21st Century; and a stronger Low than in the historical simulations (c.f. Figure 2). However, it should be noted that these MSLP distributions are for averages over a decade—so will be influenced by natural variability—in contrast to the historical average.

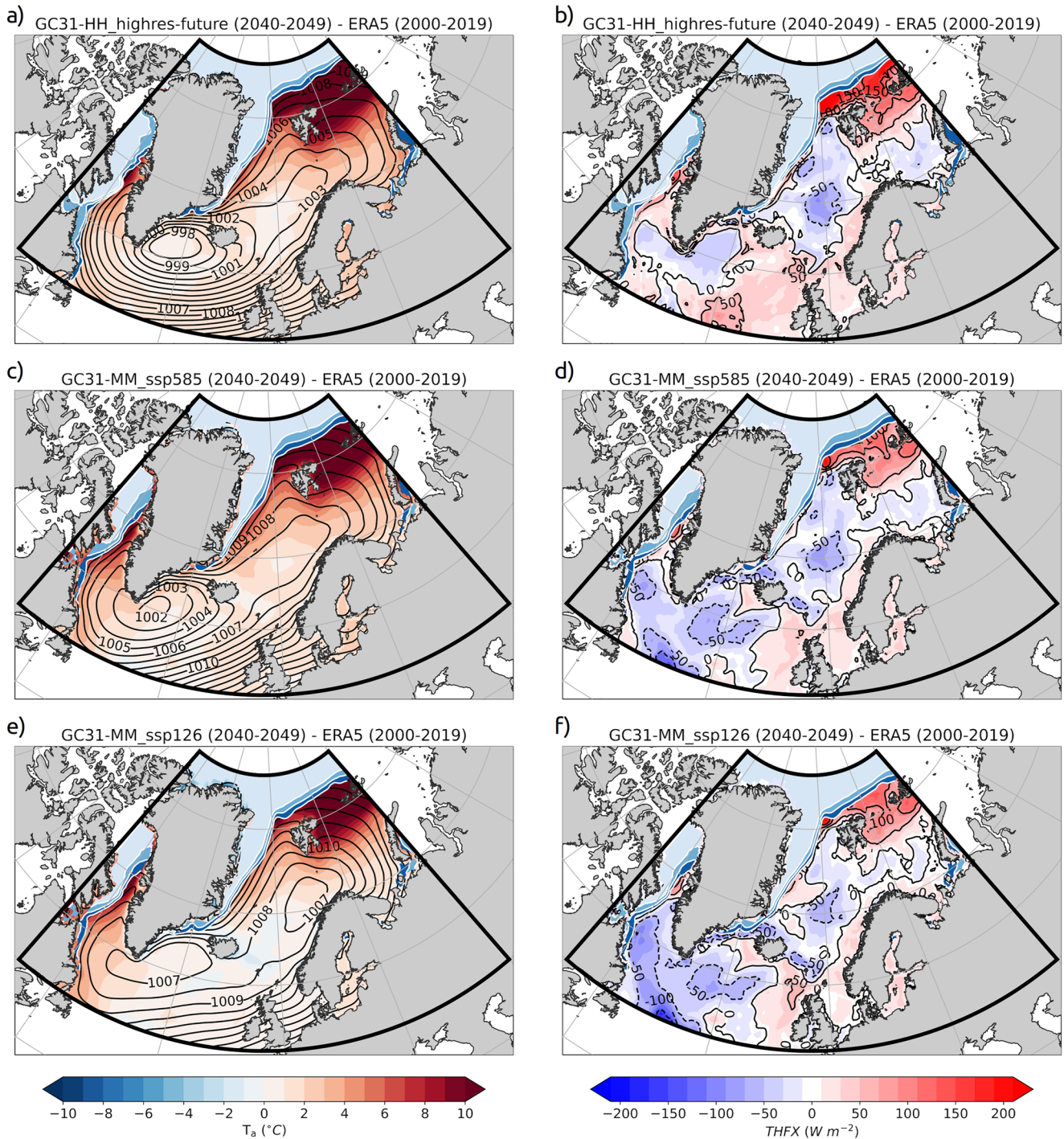


Figure 6. Spatial distribution of mean mid-century (2040–2049) sea ice concentration, sea-level pressure and 2 m air temperature anomaly (from an ERA5 “base period” between 2000 and 2019) in the left column; and sea ice concentration with total turbulent heat flux anomaly (using the same base period) in the right column. Shown for HadGEM3-GC3.1 HH future in (a) and (b); HadGEM3-GC3.1 MM SSP5-8.5 in (c) and (d); and HadGEM3-GC3.1 MM SSP1-2.6 in (e) and (f). All panels are for DJFM.

Over the interior of the SPNA winter mean THFX is projected to decrease in all of the simulations by the 2040s, by over $50 W m^{-2}$ in places (Figure 6). Conversely, to the north of Fram Strait and in the Barents Sea there is a substantial increase in THFX accompanying the sea-ice retreat and associated with a compensating reduction in THFX to the south, as cold-air outbreak airmasses will be warmer on reaching there (c.f. Moore et al., 2022).

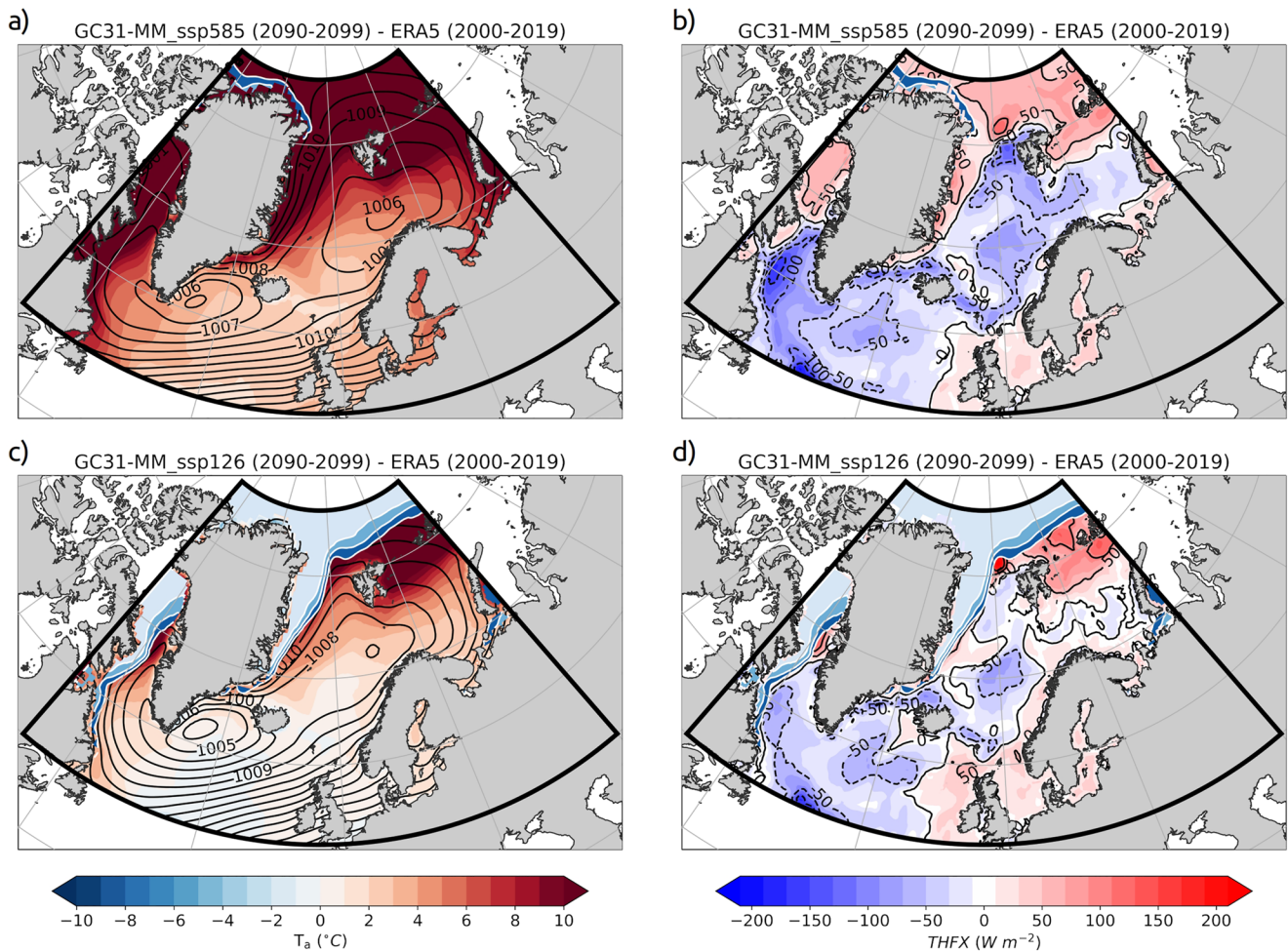


Figure 7. Spatial distribution of the late 21st century (2090–2099) sea ice, sea-level pressure with 2 m air temperature anomaly (from an ERA5 “base period” between 2000 and 2019) in the left column; and sea ice with total turbulent heat flux anomaly using the same base period in the right column. Shown for HadGEM3-GC3.1 MM SSP5-8.5 in (a) and (b); and HadGEM3-GC3.1 MM SSP1-2.6 in (c) and (d). All panels are for DJFM.

Smaller increases are projected along the Norwegian coast and where sea ice has retreated toward Greenland. The two model resolutions diverge around the Irminger and Labrador Seas, where the HH future projects only a small reduction in THFX and increases toward the coasts, while the MM simulations project a substantial and more widespread reduction under both warming scenarios. The HH and MM historic simulations were relatively similar in this region (c.f. Figure 2). For these MM projections, weaker mean winds, related to the shallower Icelandic Low, may be the primary reason for lower heat fluxes. Overall, the model simulations are qualitatively similar in their spatial distribution of sea ice and THFX, increasing confidence in the MM model's ability to project further into the future.

Late in the 21st century (2090–2099; Figure 7) the two MM simulations dramatically diverge. The high radiative forcing in SSP5-8.5 causes strong atmospheric warming and a total retreat of sea ice from the SPNA. In contrast, in the SSP1-2.6 projection there is comparatively little change between the mid- and late-21st century. This suggests that should anthropogenic emissions be kept to a minimum over this century, and atmospheric warming limited, the wintertime SPNA may reach a new state of relative equilibrium in terms of atmosphere-ocean coupling. However, under a scenario of a fossil fuel intensive economy, the MM SSP5-8.5 simulation projects a radically different regime for the SPNA with virtually no remaining wintertime sea ice, even in the “Last Ice Area” north of Greenland where the oldest and thickest sea ice typically occurs (Moore et al., 2019). In northwest Europe, the climate would be much warmer than at present, with the reduction in warming effect from a slowing AMOC outweighed by warming global mean global mean T_a (see also Liu et al., 2018; Wen et al., 2018).

In summary, substantially reduced air-sea temperature gradients in the model projections for the latter half of the 21st century result in a reduction in THFX over the majority of the SPNA, though with increased THFX where

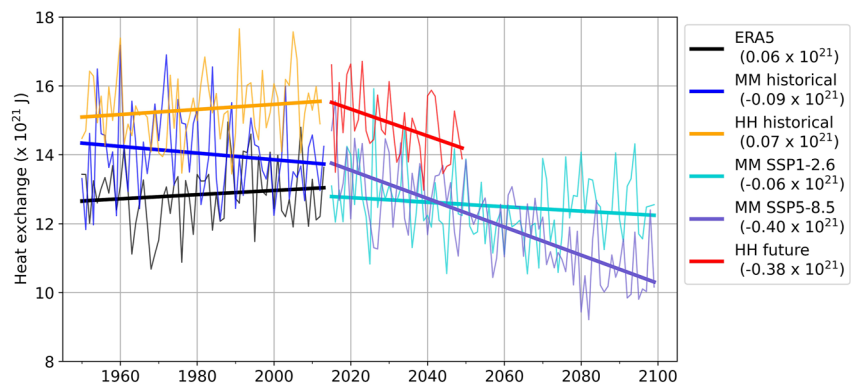


Figure 8. Time series of integrated wintertime heat exchange (positive upward) over the subpolar North Atlantic. The integrated ocean heat loss is calculated from the surface turbulent heat flux, with winter mean values (thin lines) and linear fits (thick dashed lines) shown for ERA5 (black), MM historical (blue), HH control (green), HH historical (orange), MM SSP1-2.6 (cyan), MM SSP5-8.5 (purple) and HH future (red). Decadal trend values (J decade^{-1}) are noted in the legend.

sea ice no longer exists. This translates to a substantial reduction in the atmospheric forcing of water mass transformation over most of the SPNA. After deepening in the mid-21st century, the Iceland Low in MM SSP5-8.5 at the end of the century has reduced in strength, while for MM SSP1-2.6 the reverse is true. This could be linked to the observed trend of increasing NH polar jet strength with historical climate warming over the North Atlantic Ocean (Hallam et al., 2022) and suggest that this trend may reverse later in the century, however, there is significant uncertainty with projections of changes in circulation (Harvey et al., 2020).

4.3. Integrated Turbulent Heat Fluxes

We find a projected overall decrease in the magnitude of THFX in the SPNA over the 21st century, however, large reductions in sea ice will open more of the ocean to be in direct contact with the atmosphere. Thus, a simple quantification of the total effect on overall air-sea heat exchange can be calculated by integrating every non-land grid cell in the defined SPNA region over area and time during each winter. To facilitate this calculation a common land mask from the MM model has been applied to each product. However, the absolute values are sensitive to this processing step. Likewise, the start and end points of the linear trends are sensitive to the windows chosen due to their relatively short duration. Figure 8 shows trends in the heat exchange from the 1950s–2100 from ERA5 and the historical and future simulations. It is striking that the trends in HH historical and ERA5 are similar and, under the stronger climate forcing, the projected HH and MM trends are similar. ERA5 shows a positive trend in upward air-sea heat exchange from 1950 to 2013 of $0.06 \times 10^{21} \text{ J decade}^{-1}$ linked in part to the observed reductions in sea ice extent (Moore et al., 2015, 2022), but also shown to be partly the result of increased atmospheric forcing (Li et al., 2022). This trend is simulated well in HH historical ($0.07 \times 10^{21} \text{ J decade}^{-1}$), though with higher total heat exchange due to sea ice extent that is too low in the Barents and Labrador Seas and Fram Strait (c.f. Figure 3). The HH control also simulated a heat exchange that is systematically biased high (not shown). In contrast, MM historical simulates a negative trend, though is closer to ERA5 toward the end of the simulation. We hypothesize this is linked to its initially poor representation of sea ice (e.g., its persistent Odden ice tongue) which significantly affects its THFX distribution. The HH future simulation predicts a relatively sharp decline in the heat exchange trend from THFX to 2050 ($-0.38 \times 10^{21} \text{ J decade}^{-1}$). Under the same climate forcing, MM SSP5-8.5 predicts a remarkably similar trend ($-0.40 \times 10^{21} \text{ J decade}^{-1}$), resulting in a substantial reduction in heat exchange toward 2100. The trend for MM SSP1-2.6 is also negative but is weaker. The simulated decreases in ocean heat loss are due to changes in sea-ice distribution and the temperatures of the atmosphere and ocean (as illustrated in Figures 3, 5–7). The different climate forcing scenarios directly affect the sea ice and T_a , while T_s is also affected by the declining strength of the AMOC in these simulations (Roberts et al., 2020). The implications of this reduction in ocean heat loss would be a reduction in the formation of dense waters that feed into the lower limb of the AMOC.

5. Discussion

Broadly the HH and MM historical simulations agree well with the ERA5 climatology in the subpolar North Atlantic in terms of sea ice, MSLP, T_a , T_s and THFX. However, there are substantial regional differences, largely

related to errors in the model's simulation of sea ice. The Iceland and Greenland Seas are a critical area where it is common for the models to simulate too much sea ice cover due to the overly frequent development of the Odden Ice Tongue, particularly at the MM resolution. This has a negative impact on model reproduction of the local surface atmosphere-ocean coupling. To see if the model performance is better in some scenarios, we conditionally sampled for low sea-ice years. In this low ice regime, the models benefit from smaller mean biases and reduced uncertainty stemming from reduced sea-ice variability. This suggests that for future simulations, when there is less sea ice in the SPNA, the models will be comparatively accurate.

The recent Physical Science Basis report by the Intergovernmental Panel on Climate Change (Lee et al., 2021) states that, compared to 1850–1900, global surface temperature averaged over 2081–2100 is very likely to be higher by 1.3°C–2.4°C under the low emissions scenario (SSP1-2.6), or 3.3°C–5.7°C warmer under the very high emissions scenario (SSP5-8.5). Here we show the effects of these two scenarios on sea ice and air-sea turbulent heat fluxes in the SPNA. The HH and MM simulations have been shown to project a stronger decline in the AMOC to 2050 than coarser CMIP6 models (Roberts et al., 2020). It has been suggested that this is due to a larger decrease in dense water formation in the subpolar gyre and Labrador Sea (Jackson et al., 2020). Here we show that this is concurrent with a substantial reduction in atmospheric forcing by turbulent heat fluxes.

Roberts et al. (2020) found that of the HighResMIP models, the eddy-rich HadGEM3-GC3.1 HH and CESM1-3 HH (Small et al., 2014) models reproduce AMOC depth profiles, zonal mean temperature and salinity the best. Here, we add that HadGEM3-GC3.1 HH generally produces a qualitative better sea ice and turbulent heat flux distribution for the SPNA compared to the MM configuration. However, despite the improved AMOC and hydrographic properties in the SPNA, the HH simulation has too little sea ice in the Barents Sea and north of Fram Strait. This could be linked to an increased northward heat transport and/or the accuracy of current pathways in the model. There is observational evidence of an increase in warm Atlantic water entering the Nordic Seas from 2001 onwards (Tsubouchi et al., 2020), but further investigation is required to determine how well the HH model simulates the redistribution of ocean heat energy in the SPNA.

The Odden Ice Tongue feature is known to develop in two ways: local formation of ice over the pre-cooled Jan Mayen current that splits eastward off the East Greenland Current; or advection of older ice from the coast of Greenland eastwards by the Jan Mayen current (Wadhams & Comiso, 1999). In the MM historical simulation this feature occurs too frequently, suggesting a poor representation of the current pathways and ocean heat redistribution in the region. In contrast, the inference is the HH model has a better representation of these currents.

As the global climate changes, so too will the fringe areas of sea ice. Strong and Rigor (2013) found that between 1979 and 2011 the Arctic MIZ widened by 39% in summer and narrowed by 15% in winter. With further warming the MIZ will continue to change in location and characteristics, eventually disappearing northwards from the coasts of Greenland entirely. We have found that the models perform better in winters when sea ice is reduced, giving confidence in the simulations from the 2030s onwards as sea ice becomes less prevalent in the SPNA. The projections presented suggest that wintertime sea ice later in the 21st century will be consistently closer to the Greenland coast and farther north from Svalbard. Positive winter air-sea temperature gradients, driven by cold-air outbreaks, will reduce over the 21st century, particularly under SSP5-8.5 forcing. Overall, turbulent heat fluxes decrease over the SPNA region, reducing atmospheric forcing of the ocean.

In CMIP6 models, the commonly simulated AMOC decline is often associated with a decline in North Atlantic Deep Water formation (Weijer et al., 2020). However, changes in location and magnitude of THFX maxima in the vicinity of key branches of the subpolar AMOC complicates the projected future for water mass transformation. In the western Iceland Sea, re-ventilation and a deeper mixed layer has been observed, made possible by the retreat of the ice edge in recent years (Våge et al., 2018). Furthermore, changes in sea ice near key current pathways in the Nordic and Barents Seas has been shown to be affecting where and how water mass transformation occurs (Moore et al., 2022). Over the East Greenland Current a significant increase in THFX has been observed since 1950 due to the current's orientation being perpendicular to the axis of sea ice retreat, exposing the entire current system to the cold atmosphere as the ice has retreated; however, the northward flowing currents to the west of Svalbard and in the Barents Sea have seen a dipolar change in THFX along the current length due to their orientation parallel to the axis of sea ice retreat (Moore et al., 2022). Here we show that this pattern of THFX changes due to sea-ice loss over these key currents is expected to continue in the future, though local increases will be dwarfed by a background reduction in THFX over the SPNA due to differential warming in the atmosphere and the ocean under strong anthropogenic climate forcing.

Higher resolution atmospheric models typically perform better, in part due to more realistic orography (Jung et al., 2012). This issue is pertinent for the SPNA due to the large barrier of Greenland that influences large-scale atmospheric circulation and generates smaller-scale phenomena, such as topographic jets and mesoscale cyclones. Further, improved representation of mesoscale atmospheric forcing on the ocean in a high-resolution atmosphere model has been shown to increase the strength of wind-driven gyres in the North Atlantic and the AMOC by around 5%–10% (Jung et al., 2014) and increase water mass transformation (Condrón & Renfrew, 2013). We illustrate that the Icelandic Low is more accurately reproduced by the HH model. The HH future simulation suggests a 2 hPa deepening of the Icelandic low by the 2040s, while the MM simulations predict that it will become shallower by the end of the 21st century. Although these are single realizations; in projections from the CMIP6 ensemble, it has been suggested that the NAO will not change substantially in respect to historical conditions (Cusinato et al., 2021).

6. Conclusions

We evaluate historical simulations from the HadGEM3-GC3.1 model at medium-medium resolution (MM; 60 km atmosphere—1/4° ocean) and high-high resolution (HH; 25 km—1/12°), finding that both show reasonably good spatial agreement in sea ice and total surface turbulent heat fluxes (THFX) over the subpolar North Atlantic (SPNA). Overall, the HH model performs better than the MM, mainly due to a more representative ocean and more accurate sea ice. A particular problem for the MM historic is the simulation of too much sea ice in the Iceland and Greenland Seas, resulting in an inaccurate THFX distribution there. Our results demonstrate that the representation of sea ice is a major source of model variability and error in the SPNA. However, when conditionally sampling the MM historic output for winters with low ice extent in the SPNA, we show that its performance is improved in winters with less sea ice in the Iceland and Greenland Seas, which increases confidence in future projections as sea ice declines.

We show that winter sea ice is projected to substantially reduce in the SPNA over the 21st century, particularly under the high greenhouse gas emissions scenario, SSP5-8.5. This will affect the location and magnitude of peak turbulent heat fluxes, generally tracking the ice edge poleward. Also, rapid warming of the atmosphere will reduce the air-sea temperature gradient and the extraction of heat from the ocean. We find a negative trend in THFX in the Labrador Sea, Irminger Sea, and interior of the Nordic Seas. Under low emissions forcing (SSP1-2.6), these reductions in sea ice and changes to air-sea interactions are less severe than under high emissions forcing (SSP5-8.5), but still considerable.

Reduced THFX in winter will reduce the formation rate of dense waters that feed into the AMOC. This has the potential to compound the decreasing strength of the AMOC seen in recent years, with greater impacts possible from climate warming. However, changes in the position of THFX maxima near key ocean currents, such as over the East Greenland current (as it is increasingly exposed to the atmosphere), will have more complicated impacts on water mass transformation that require further investigation. Future work should also include investigation into the accuracy of AMOC pathways in high resolution models, specifically the inflows and outflows of the Nordic Seas basin and the mechanisms by which ocean heat is redistributed around the SPNA.

Data Availability Statement

The HadGEM3-GC3.1 simulation data used in this study is available from the Centre for Environmental Data Analysis (HH: <https://data.ceda.ac.uk/badc/cmip6/data/CMIP6/HighResMIP/MOHC>; MM: <https://data.ceda.ac.uk/cmip6/data/CMIP6/CMIP/MOHC>) and ERA5 reanalysis data is available via the Copernicus Climate Change Service Climate Data Store (<https://climate.copernicus.eu/climate-reanalysis>).

References

- Aagaard, K., & Carmack, E. C. (1989). The role of sea ice and other fresh-water in the Arctic Circulation. *Journal of Geophysical Research*, 94(C10), 14485–14498. <https://doi.org/10.1029/JC094iC10p14485>
- Andrews, M., Ridley, J., Wood, R., Andrews, T., Blockley, E., Booth, B., et al. (2020). Historical simulations with HadGEM3-GC3.1 for CMIP6. *Journal of Advances in Modeling Earth Systems*, 12(6), e2019MS001995. <https://doi.org/10.1029/2019ms001995>
- Bell, B., Hersbach, H., Berrisford, P., Dahlgren, P., Horányi, A., Muñoz Sabater, J., et al. (2020). ERA5 monthly averaged data on single levels from 1950 to 1978 (preliminary version). *Copernicus Climate Change Service (C3S) Climate Data Store (CDS)*.

Acknowledgments

This study was part of the Iceland Greenland Seas Project, supported by the Natural Environmental Research Council (NERC) AFIS Grant (NE/N009754/1). This work was also supported by NERC via the EnvEast DTP (Grant NE/L002582/1). The authors acknowledge the UK Met Office Hadley Centre modelling group and others who contributed to the HadGEM3-GC3.1 climate model, supported by NERC. Model data was accessed from the Centre for Environmental Data Analysis (CEDA) using the JASMIN supercomputing service (<https://www.jasmin.ac.uk>). The authors also acknowledge the European Centre for Medium-Range Weather Forecasts (ECMWF) for providing the ERA5 reanalysis data set. We'd like to thank the reviewers for comments that have improved the final paper.

- Buckley, M. W., & Marshall, J. (2016). Observations, inferences, and mechanisms of the Atlantic meridional overturning circulation: A review. *Reviews of Geophysics*, 54(1), 5–63. <https://doi.org/10.1002/2015RG000493>
- Caesar, L., Rahmstorf, S., Robinson, A., Feulner, G., & Saba, V. (2018). Observed fingerprint of a weakening Atlantic Ocean overturning circulation. *Nature*, 556(7700), 191–196. <https://doi.org/10.1038/s41586-018-0006-5>
- Cavalieri, D., & Parkinson, C. (2012). Arctic sea ice variability and trends, 1979–2010. *The Cryosphere*, 6(4), 881–889. <https://doi.org/10.5194/tc-6-881-2012>
- Chassignet, E. P., Yeager, S. G., Fox-Kemper, B., Bozec, A., Castruccio, F., Danabasoglu, G., et al. (2020). Impact of horizontal resolution on global ocean–sea ice model simulations based on the experimental protocols of the Ocean Model Intercomparison Project phase 2 (OMIP-2). *Geoscientific Model Development*, 13(9), 4595–4637. <https://doi.org/10.5194/gmd-13-4595-2020>
- Comiso, J. C., Parkinson, C. L., Gersten, R., & Stock, L. (2008). Accelerated decline in the Arctic sea ice cover. *Geophysical Research Letters*, 35(1), L01703. <https://doi.org/10.1029/2007gl031972>
- Condron, A., & Renfrew, I. A. (2013). The impact of polar mesoscale storms on northeast Atlantic Ocean circulation. *Nature Geoscience*, 6(1), 34–37. <https://doi.org/10.1038/ngeo1661>
- Cusinato, E., Rubino, A., & Zanchettin, D. (2021). Winter Euro-Atlantic climate modes: Future scenarios from a CMIP6 multi-model ensemble. *Geophysical Research Letters*, 48(19), e2021GL094532. <https://doi.org/10.1029/2021gl094532>
- Elvidge, A. D., Renfrew, I. A., Brooks, I. M., Srivastava, P., Yelland, M. J., & Prytherch, J. (2021). Surface heat and moisture exchange in the marginal ice zone: Observations and a new parameterization scheme for weather and climate models. *Journal of Geophysical Research: Atmospheres*, 126(17), e2021JD034827. <https://doi.org/10.1029/2021jd034827>
- Elvidge, A. D., Renfrew, I. A., Weiss, A. I., Brooks, I. M., Lachlan-Cope, T. A., & King, J. C. (2016). Observations of surface momentum exchange over the marginal ice zone and recommendations for its parametrisation. *Atmospheric Chemistry and Physics*, 16(3), 1545–1563. <https://doi.org/10.5194/acp-16-1545-2016>
- Eyring, V., Bony, S., Meehl, G. A., Senior, C. A., Stevens, B., Stouffer, R. J., & Taylor, K. E. (2016). Overview of the Coupled Model Intercomparison Project Phase 6 (CMIP6) experimental design and organization. *Geoscientific Model Development*, 9(5), 1937–1958. <https://doi.org/10.5194/gmd-9-1937-2016>
- Fox-Kemper, B., Hewitt, H. T., Xiao, C., Aðalgeirsdóttir, G., Drijfhout, S. S., Edwards, T. L., et al. (2021). Ocean, cryosphere and sea level change. In V. Masson-Delmotte, P. Zhai, A. Pirani, S. L. Connors, C. Péan, S. Berger, et al. (Eds.), *Climate change 2021: The physical science basis. Contribution of working Group I to the sixth assessment report of the intergovernmental panel on climate change*. Cambridge University Press.
- Graham, R. M., Cohen, L., Ritzhaupt, N., Segger, B., Graverson, R. G., Rinke, A., et al. (2019). Evaluation of six atmospheric reanalyses over Arctic sea ice from winter to early summer. *Journal of Climate*, 32(14), 4121–4143. <https://doi.org/10.1175/jcli-d-18-0643.1>
- Haarsma, R. J., Roberts, M. J., Vidale, P. L., Senior, C. A., Bellucci, A., Bao, Q., et al. (2016). High resolution model intercomparison project (HighResMIP v1.0) for CMIP6. *Geoscientific Model Development*, 9(11), 4185–4208. <https://doi.org/10.5194/gmd-9-4185-2016>
- Hallam, S., Josey, S., McCarthy, G., & Hirschi, J. (2022). A regional (land–ocean) comparison of the seasonal to decadal variability of the Northern Hemisphere jet stream 1871–2011. *Climate Dynamics*, 59(7–8), 1897–1918. <https://doi.org/10.1007/s00382-022-06185-5>
- Harvey, B. J., Cook, P., Shaffrey, L. C., & Schiemann, R. (2020). The response of the northern hemisphere storm tracks and jet streams to climate change in the CMIP3, CMIP5, and CMIP6 climate models. *Journal of Geophysical Research: Atmospheres*, 125(23), e2020JD032701. <https://doi.org/10.1029/2020jd032701>
- Hersbach, H., Bell, B., Berrisford, P., Biavati, G., Horányi, A., Muñoz Sabater, J., et al. (2019). ERA5 monthly averaged data on single levels from 1979 to present. *Copernicus Climate Change Service (C3S) Climate Data Store (CDS)*.
- Heuzé, C. (2021). Antarctic bottom water and North Atlantic deep water in CMIP6 models. *Ocean Science*, 17(1), 59–90. <https://doi.org/10.5194/os-17-59-2021>
- Hirschi, J. J., Barnier, B., Böning, C., Biastoch, A., Blaker, A. T., Coward, A., et al. (2020). The Atlantic meridional overturning circulation in high-resolution models. *Journal of Geophysical Research: Oceans*, 125(4), e2019JC015522. <https://doi.org/10.1029/2019jc015522>
- IPCC. (2021). In V. Masson-Delmotte, P. Zhai, A. Pirani, S. L. Connors, C. Péan, et al. (Eds.), *Climate change 2021: The physical science basis. Contribution of working Group I to the sixth assessment report of the intergovernmental panel on climate change*. Cambridge University Press.
- Jackson, L. C., Roberts, M. J., Hewitt, H. T., Iovino, D., Koenigk, T., Meccia, V. L., et al. (2020). Impact of ocean resolution and mean state on the rate of AMOC weakening. *Climate Dynamics*, 55(7–8), 1711–1732. <https://doi.org/10.1007/s00382-020-05345-9>
- Jung, T., Gulev, S., Rudeva, I., & Soloviev, V. (2006). Sensitivity of extratropical cyclone characteristics to horizontal resolution in the ECMWF model. *Quarterly Journal of the Royal Meteorological Society*, 132(619), 1839–1857. <https://doi.org/10.1256/qj.05.212>
- Jung, T., Miller, M. J., Palmer, T. N., Towers, P., Wedi, N., Achuthavarier, D., et al. (2012). High-resolution global climate simulations with the ECMWF model in project Athena: Experimental design, model climate, and seasonal forecast skill. *Journal of Climate*, 25(9), 3155–3172. <https://doi.org/10.1175/JCLI-D-11-00265.1>
- Jung, T., Serrar, S., & Wang, Q. (2014). The oceanic response to mesoscale atmospheric forcing. *Geophysical Research Letters*, 41(4), 1255–1260. <https://doi.org/10.1002/2013gl059040>
- Keen, A., Blockley, E., Bailey, D. A., Bolding Debernard, J., Bushuk, M., Delhaye, S., et al. (2021). An inter-comparison of the mass budget of the Arctic sea ice in CMIP6 models. *The Cryosphere*, 15(2), 951–982. <https://doi.org/10.5194/tc-15-951-2021>
- Lee, J.-Y., Marotzke, J., Bala, G., Cao, L., Corti, S., Dunne, J. P., et al. (2021). Future global climate: Scenario-based projections and near-term information. In V. Masson-Delmotte, P. Zhai, A. Pirani, S. L. Connors, C. Péan, S. Berger, et al. (Eds.), *Climate change 2021: The physical science basis. Contribution of working Group I to the sixth assessment report of the intergovernmental panel on climate change*. Cambridge University Press.
- Li, L., Lozier, M. S., & Li, F. (2022). Century-long cooling trend in subpolar North Atlantic forced by atmosphere: An alternative explanation. *Climate Dynamics*, 58(9–10), 2249–2267. <https://doi.org/10.1007/s00382-021-06003-4>
- Liu, Y., Hallberg, R., Sergienko, O., Samuels, B. L., Harrison, M., & Oppenheimer, M. (2018). Climate response to the meltwater runoff from Greenland ice sheet: Evolving sensitivity to discharging locations. *Climate Dynamics*, 51(5), 1733–1751. <https://doi.org/10.1007/s00382-017-3980-7>
- Moore, G. W. K., Renfrew, I. A., & Pickart, R. S. (2012). Spatial distribution of air–sea heat fluxes over the sub-polar North Atlantic Ocean. *Geophysical Research Letters*, 39(18), L18806. <https://doi.org/10.1029/2012gl053097>
- Moore, G. W. K., Schweiger, A., Zhang, J., & Steele, M. (2019). Spatiotemporal variability of sea ice in the Arctic's last ice area. *Geophysical Research Letters*, 46(20), 11237–11243. <https://doi.org/10.1029/2019gl083722>
- Moore, G. W. K., Våge, K., Pickart, R. S., & Renfrew, I. A. (2015). Decreasing intensity of open-ocean convection in the Greenland and Iceland seas. *Nature Climate Change*, 5(9), 877–882. <https://doi.org/10.1038/nclimate2688>

- Moore, G. W. K., Våge, K., Renfrew, I. A., & Pickart, R. S. (2022). Sea-ice retreat suggests re-organization of water mass transformation in the Nordic and Barents Seas. *Nature Communications*, *13*(1), 1–8. <https://doi.org/10.1038/s41467-021-27641-6>
- Notz, D., & SIMIP Community. (2020). Arctic sea ice in CMIP6. *Geophysical Research Letters*, *47*, e2019GL086749. <https://doi.org/10.1029/2019GL086749>
- Overland, J. E., & Wang, M. (2013). When will the summer Arctic be nearly sea ice free? *Geophysical Research Letters*, *40*(10), 2097–2101. <https://doi.org/10.1002/grl.50316>
- Palmer, J. B. (2015). The role of the Gulf Stream in European climate. In C. A. Carlson & S. J. Giovannoni (Eds.), *Annual review of marine science* (Vol. 7, pp. 113–137).
- Papritz, L., & Spengler, T. (2017). A Lagrangian climatology of wintertime cold air outbreaks in the Irminger and Nordic seas and their role in shaping air–sea heat fluxes. *Journal of Climate*, *30*(8), 2717–2737. <https://doi.org/10.1175/jcli-d-16-0605.1>
- Parkinson, C. L., & Cavalieri, D. J. (2008). Arctic sea ice variability and trends, 1979–2006. *Journal of Geophysical Research*, *113*(C7), C07003. <https://doi.org/10.1029/2007JC004558>
- Rahmstorf, S., Box, J. E., Feulner, G., Mann, M. E., Robinson, A., Rutherford, S., & Schaffernicht, E. J. (2015). Exceptional twentieth-century slowdown in Atlantic Ocean overturning circulation. *Nature Climate Change*, *5*(5), 475–480. <https://doi.org/10.1038/nclimate2554>
- Renfrew, I. A., Barrell, C., Elvidge, A. D., Brooke, J. K., Duscha, C., King, J. C., et al. (2021). An evaluation of surface meteorology and fluxes over the Iceland and Greenland Seas in ERA5 reanalysis: The impact of sea ice distribution. *Quarterly Journal of the Royal Meteorological Society*, *147*(734), 691–712. <https://doi.org/10.1002/qj.3941>
- Renfrew, I. A., Elvidge, A. D., & Edwards, J. M. (2019). Atmospheric sensitivity to marginal-ice-zone drag: Local and global responses. *Quarterly Journal of the Royal Meteorological Society*, *145*(720), 1165–1179. <https://doi.org/10.1002/qj.3486>
- Ridley, J. K., Blockley, E. W., Keen, A. B., Rae, J. G. L., West, A. E., & Schroeder, D. (2018). The sea ice model component of HadGEM3-GC3.1. *Geoscientific Model Development*, *11*(2), 713–723. <https://doi.org/10.5194/gmd-11-713-2018>
- Roberts, M. (2017). MOHC HadGEM3-GC31-HH model output prepared for CMIP6 HighResMIP, Earth system grid federation. Retrieved from <http://cera-www.dkrz.de/WDCC/meta/CMIP6/CMIP6.HighResMIP.MOHC.HadGEM3-GC31-HH>
- Roberts, M., Baker, A., Blockley, E. W., Calvert, D., Coward, A., Hewitt, H. T., et al. (2019). Description of the resolution hierarchy of the global coupled HadGEM3-GC3.1 model as used in CMIP6 HighResMIP experiments. *Geoscientific Model Development*, *12*(12), 4999–5028. <https://doi.org/10.5194/gmd-12-4999-2019>
- Roberts, M. J., Jackson, L. C., Roberts, C. D., Meccia, V., Docquier, D., Koenig, T., et al. (2020). Sensitivity of the Atlantic meridional overturning circulation to model resolution in CMIP6 HighResMIP simulations and implications for future changes. *Journal of Advances in Modeling Earth Systems*, *12*(8), e2019MS002014. <https://doi.org/10.1029/2019ms002014>
- Schmitz, W. J. (1995). On the interbasin-scale thermohaline circulation. *Reviews of Geophysics*, *33*(2), 151–173. <https://doi.org/10.1029/95rg00879>
- Serreze, M., & Barry, R. (2011). Processes and impacts of Arctic amplification: A research synthesis. *Global and Planetary Change*, *77*(1–2), 85–96. <https://doi.org/10.1016/j.gloplacha.2011.03.004>
- Sévellec, F., Fedorov, A., & Liu, W. (2017). Arctic sea-ice decline weakens the Atlantic meridional overturning circulation. *Nature Climate Change*, *7*(8), 604–610. <https://doi.org/10.1038/nclimate3353>
- Shepherd, T. G., Boyd, E., Calel, R. A., Chapman, S. C., Dessai, S., Dima-West, I. M., et al. (2018). Storylines: An alternative approach to representing uncertainty in physical aspects of climate change. *Climatic Change*, *151*(3–4), 555–571. <https://doi.org/10.1007/s10584-018-2317-9>
- Small, R. J., Bacmeister, J., Bailey, D., Baker, A., Bishop, S., Bryan, F., et al. (2014). A new synoptic scale resolving global climate simulation using the Community Earth System Model. *Journal of Advances in Modeling Earth Systems*, *6*(4), 1065–1094. <https://doi.org/10.1002/2014MS000363>
- Smeed, D. A., Josey, S. A., Beaulieu, C., Johns, W. E., Moat, B. I., Frajka-Williams, E., et al. (2018). The North Atlantic Ocean is in a state of reduced overturning. *Geophysical Research Letters*, *45*(3), 1527–1533. <https://doi.org/10.1002/2017gl076350>
- Storkey, D., Blaker, A. T., Mathiot, P., Megann, A., Aksenov, Y., Blockley, E. W., et al. (2018). UK Global Ocean GO6 and GO7: A traceable hierarchy of model resolutions. *Geoscientific Model Development*, *11*(8), 3187–3213. <https://doi.org/10.5194/gmd-11-3187-2018>
- Strong, C., & Rigor, I. (2013). Arctic marginal ice zone trending wider in summer and narrower in winter. *Geophysical Research Letters*, *40*(18), 4864–4868. <https://doi.org/10.1002/grl.50928>
- Talley, L. (1996). North Atlantic circulation and variability, reviewed for the CNLS conference. *Physica D: Nonlinear Phenomena*, *98*(2–4), 625–646. [https://doi.org/10.1016/0167-2789\(96\)00123-6](https://doi.org/10.1016/0167-2789(96)00123-6)
- Tsubouchi, T., Våge, K., Hansen, B., Larsen, K. M. H., Østerhus, S., Johnson, C., et al. (2020). Increased ocean heat transport into the Nordic seas and Arctic Ocean over the period 1993–2016. *Nature Climate Change*, *11*(1), 21–26. <https://doi.org/10.1038/s41558-020-00941-3>
- Våge, K., Papritz, L., Håvik, L., Spall, M. A., & Moore, G. W. K. (2018). Ocean convection linked to the recent ice edge retreat along east Greenland. *Nature Communications*, *9*(1), 1287. <https://doi.org/10.1038/s41467-018-03468-6>
- Wadhams, P., & Comiso, J. C. (1999). Two modes of appearance of the Odden ice tongue in the Greenland Sea. *Geophysical Research Letters*, *26*(16), 2497–2500. <https://doi.org/10.1029/1999gl900502>
- Walters, D., Baran, A. J., Boutle, I., Brooks, M., Earnshaw, P., Edwards, J., et al. (2019). The met office unified model global atmosphere 7.0/7.1 and JULES global land 7.0 configurations. *Geoscientific Model Development*, *12*(5), 1909–1963. <https://doi.org/10.5194/gmd-12-1909-2019>
- Wang, Q., Wekerle, C., Wang, X., Danilov, S., Koldunov, N., Sein, D., et al. (2020). Intensification of the Atlantic water supply to the Arctic Ocean through Fram Strait induced by Arctic sea ice decline. *Geophysical Research Letters*, *47*(3), e2019GL086682. <https://doi.org/10.1029/2019gl086682>
- Weijer, W., Cheng, W., Garuba, O. A., Hu, A., & Nadiga, B. T. (2020). CMIP6 models predict significant 21st century decline of the Atlantic meridional overturning circulation. *Geophysical Research Letters*, *47*(12), e2019GL086075. <https://doi.org/10.1029/2019gl086075>
- Wen, Q., Yao, J., Döös, K., & Yang, H. (2018). Decoding hosing and heating effects on global temperature and meridional circulations in a warming Climate. *Journal of Climate*, *31*(23), 9605–9623. <https://doi.org/10.1175/jcli-d-18-0297.1>
- Williams, K. D., Copsey, D., Blockley, E. W., Bodas-Salcedo, A., Calvert, D., Comer, R., et al. (2017). The Met Office Global Coupled model 3.0 and 3.1 (GC3.0 and GC3.1) configurations. *Journal of Advances in Modeling Earth Systems*, *10*(2), 357–380. <https://doi.org/10.1002/2017MS001115>
- Zhang, R., Sutton, R., Danabasoglu, G., Kwon, Y.-O., Marsh, R., Yeager, S. G., et al. (2019). A review of the role of the Atlantic meridional overturning circulation in Atlantic multidecadal variability and associated climate impacts. *Reviews of Geophysics*, *57*(2), 316–375. <https://doi.org/10.1029/2019RG000644>